Chapter 11

Microscale Thermophoresis Analysis of Chromatin Interactions

Ivan Corbeski, Velten Horn, Ramon A. van der Valk, Ulric B. le Paige, Remus T. Dame, and Hugo van Ingen

Abstract

Architectural DNA-binding proteins are key to the organization and compaction of genomic DNA inside cells. The activity of architectural proteins is often subject to further modulation and regulation through the interaction with a diverse array of other protein factors. Detailed knowledge on the binding modes involved is crucial for our understanding of how these protein-protein and protein-DNA interactions shape the functional landscape of chromatin in all kingdoms of life: bacteria, archaea, and eukarya.

Microscale thermophoresis (MST) is a biophysical technique that has seen increasing application in the study of biomolecular interactions thanks to its solution-based nature, its rapid application, modest sample demand, and the sensitivity of the thermophoresis effect to binding events. Here, we describe the use of MST in the study of chromatin interactions, with emphasis on the wide range of ways in which these experiments are set up and the diverse types of information they reveal. These aspects are illustrated with four very different systems: the sequence-dependent DNA compaction by architectural protein HMfB; the sequential binding of core histone complexes to histone chaperone APLF; the impact of the nucleosomal context on the recognition of histone modifications; and the binding of a LANA-derived peptide to nucleosome core. Special emphasis is given to the key steps in the design, execution, and analysis of MST experiments in the context of the provided examples.

Key words MST, HMf, Nucleosome, Histones, DNA, Binding affinity

1 Introduction

Biophysical characterization of functional chromatin interactions has typically relied thus far on band-shift assays (electrophoretic mobility shift assays, EMSA) for protein-DNA interaction, as well as on common biophysical techniques such as surface plasmon resonance (SPR), isothermal calorimetry (ITC), and nuclear magnetic resonance (NMR). Thorough characterization of binding modes and binding affinities is often a critical step preceding

Ivan Corbeski and Velten Horn contributed equally to this work.

Remus T. Dame (ed.), *Bacterial Chromatin: Methods and Protocols*, Methods in Molecular Biology, vol. 1837,
https://doi.org/10.1007/978-1-4939-8675-0_11,

subsequent structural and functional studies. This calls for a flexible technique which is fast and can characterize interactions in solution with reasonable throughput and modest sample demands. Microscale thermophoresis (MST) fulfills these criteria and thus provides an efficient option for the analysis of biological interactions.

1.1 MST

Analogous to electrophoresis, thermophoresis is the flow or directed movement of molecules along a temperature gradient [1]. Technological advances have made it possible to use small temperature gradients (typically 2–6 °C) and detect the resulting micrometer-scale movements, allowing the application in molecular biology as microscale thermophoresis (MST) [2]. MST typically requires fluorescent labeling of the protein of interest for high sensitivity of detection. Samples are loaded onto glass capillaries and a specific spot is heated by an infra-red laser (*see* Fig. 1a). The resulting temperature gradient causes thermophoresis of the labeled molecule, typically away from the heated spot, which is observed through a decrease in fluorescence in the heated region (*see* Fig. 1b). Since thermophoresis is sensitive to molecular size, charge, and hydration shell [3], changes in these properties due to binding will cause changes in thermophoresis. For analysis of interactions, MST curves are recorded as titration series with increasing amounts of ligand and normalized with respect to their initial equilibrium fluorescence (F_{norm}) (Fig. 1b). A binding curve is extracted by plotting the F_{norm} values at the end of the laser on –period (phase IV, Fig. 1b), which captures binding induced changes both in thermophoresis and in the intrinsic temperature dependence of the fluorophore (indicated by the arrow "Thermophoresis + T-Jump" in Fig. 1b). Both effects can also be analyzed separately. Since the observed F_{norm} values are the population weighted averages of the unbound and bound molecules, standard methods can be used to fit the binding curve and extract the binding affinity. Furthermore, MST can be performed in virtually every buffer [4] and other characteristics such as thermodynamic properties, binding stoichiometry, and enzyme kinetics can be extracted with customized experimental designs [5].

1.2 MST of Chromatin Systems

The study of chromatin function is strongly connected to DNA-protein and protein-protein interactions that modulate the chromatin state. An increasing number of studies has employed MST to investigate binding events in chromatin related systems (*see* for instance [6–10]), and some of the earliest examples have been included in reviews [11–14]. A variety of labeling strategies have emerged, in particular for the study of nucleosome-protein interactions. Fluorescent nucleosomes have been constructed using Cy5-labeled DNA [14], or AlexaFluor647-labeled histone H3 [15]. Furthermore, MST has been used to derive insights in protein-binding mechanisms, e.g., demonstration of cooperative

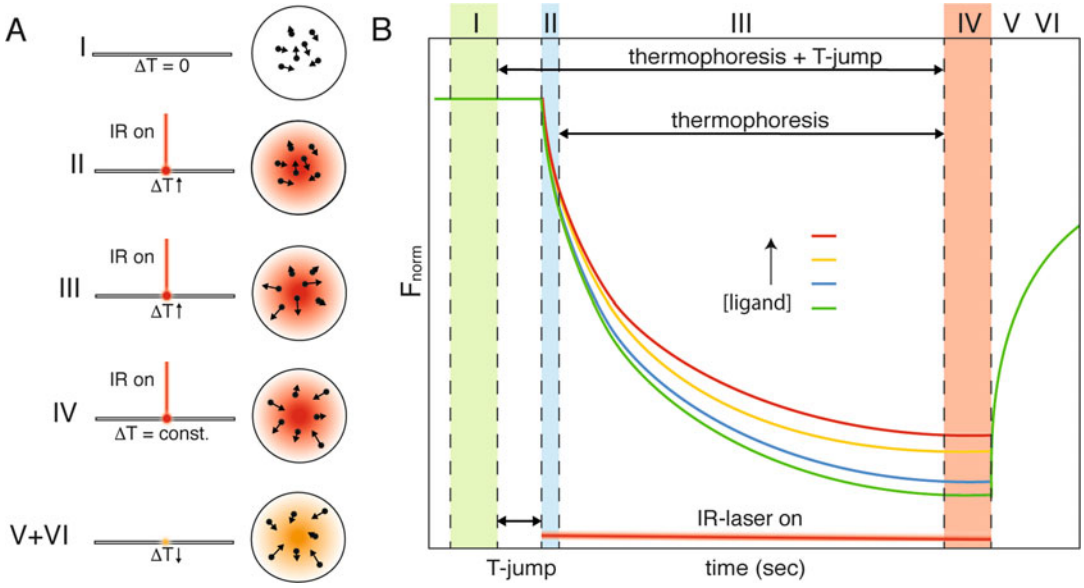

Fig. 1 Principle of MST. Schematic depiction of the MST experiment (**a**) and MST time trace (**b**). In (**a**), the capillaries (left) and particles in a cross-section thereof (right) during different stages of the experiment (I–VI) are shown. Starting from equilibrium (phase I), laser irradiation is started (phase II), causing particles to move out or into the heated volume (thermophoresis, phase III). When thermophoresis is counter balanced by mass diffusion a steady state is reached (phase IV). When the laser is switched off, the particle concentration re-equilibrates (phase VI). In (**b**), a four-sample titration series is shown, ligand concentration indicated. Each sample is characterized by a distinct thermophoresis curve. The rapid change in normalized fluorescence in phases II and V is caused by the temperature dependence in fluorescence (T-jump). Binding curves can be extracted by plotting F_{norm} values for regions "Thermophoresis + T-jump" (I vs. IV), Thermophoresis (start vs. end of III), or T-jump (I vs. II)

binding [16] or determination of binding sites from a comparison of different deletion mutants [17].

Here, we describe in detail the use of MST to study chromatin interactions. We put particular emphasis on the step-by-step optimization of experimental conditions. We present examples on the interaction of architectural proteins with both DNA and other proteins, which illustrate the additional information MST can provide on the binding mechanism, the sensitivity of the thermophoretic effect, and the merits of custom data analysis. With these, we provide first-hand reports on assay issues observed for various chromatin-related samples and strategies to detect and overcome them.

2 Materials

2.1 Fluorescent Labeling

1. Monolith NT™ Protein Labeling Kit RED/GREEN/BLUE, either NT-647-NHS, which reacts with solvent exposed primary amines, or NT-647-MALEIMIDE which reacts with

sulfhydryl groups to form dye-protein conjugates (NanoTemper Technologies) (*see* **Note 1**).

2. Variable speed benchtop microcentrifuge.
3. 1.5–2 mL microcentrifuge tubes.
4. 10 mL assay buffer (*see* **Note 2**).
5. 100% dimethylsulfoxide (DMSO).
6. Eppendorf heating block capable of reaching 95 °C (for the preparation of labeled dsDNA only).

Prepare all solutions using water (resistivity 18.2 MΩ × cm and organic content less than five parts per billion) and analytical grade reagents.

2.2 MST

1. MST instrument Monolith NT.115 equipped with "Red" channel (NanoTemper Technologies) (*see* **Note 3**).
2. Capillaries: NT.115 standard, hydrophobic, hydrophilic (*see* **Note 4**) or premium treated capillaries, or the NT.115™ Capillary Selection Set (NanoTemper Technologies).
3. PC with dedicated NT Control and MO Affinity Analysis software (version 2.1.5). Custom analysis scripts are available upon request from the corresponding author.
4. Small volume reaction tubes (e.g., as found in the labeling kit or 200 μL PCR tubes).
5. Calibrated pipettes in the range 2–1000 μL.
6. NanoDrop™ Spectrophotometer (Thermo Scientific).
7. Aluminum foil.

2.3 Stock Solutions

1. At least 100 μL of 20 μM of biomolecule to be labeled (*see* **Note 5**).
2. 100 μL of biomolecule to be titrated with a concentration 20 times the expected dissociation constant (*see* **Note 5**).
3. 10 mL of assay buffer.
4. 10–100 mg/mL bovine serum albumin (BSA).
5. 5–10% Tween-20.
6. 4 M NaCl.

3 Methods

3.1 Design of MST Experiment: Choice of Fluorescent Labeling

The MST experiment can be performed with either of the interaction partners fluorescently labeled (*see* **Note 6**). Proteins and peptides can be labeled either with the manufacturer's labeling kits or with other widely available fluorophores and coupling strategies (*see* also **Note 1**). DNA molecules are readily labeled using custom

oligo synthesis using commercially available labeled nucleotides, or using modification of the termini for coupling of dyes. For the applications described below, proteins were labeled using the manufacturer supplied labeling kits, as detailed in Subheading 3.1.1, labeling of DNA is described in Subheading 3.1.2.

3.1.1 Protein Labeling

1. Prepare a solution of pure protein at a concentration of 20 μM in a volume of 100 μL.
2. Prepare the spin column for buffer exchange into labeling buffer, using the manufacturer supplied spin columns and instructions (*see* **Note 7**). Resuspend the dried labeling buffer in 3.0 mL water. Prepare column A by resuspending the slurry. Remove excess storage solution by placing the column in a 1.5–2 mL microcentrifuge tube and centrifuging at 1500 × *g* for 1 min. Wash the column three times with 300 μL labeling buffer.
3. Exchange the protein to labeling buffer by placing the protein solution from **step 1** at the center of the resin. Be careful not to disturb the resin. Place the column in a new microcentrifuge tube and centrifuge at 1500 × *g* for 2 min.
4. Dissolve the solid fluorescent dye in 30 μL DMSO (yielding a ~470 μM solution) and mix thoroughly by vortexing (*see* **Note 8**). Prepare 100 μL 20–60 μM dye solution in Labeling Buffer (*see* **Note 9**) and take 100 μL 20 μM protein solution in Labeling Buffer. Add the dye to the protein in a 1:1 volume ratio for a final 1:1–3:1 molar ratio of dye to protein in a 200 μL volume. Incubate the reaction for 30 min at room temperature and in the dark (*see* **Note 10**). Proceed with **step 5** in the meantime.
5. Prepare the gravity flow column for purification of labeled protein and removal of unreacted dye (*see* **Note 11**). Pour off the storage solution in column B and wash the column three times with 3 mL assay buffer (*see* **Note 2**) in a 15 mL tube using the supplied adapter through gravity flow.
6. Separate the labeled protein obtained at **step 4** from unreacted dye. Apply the labeling reaction mixture to the center of column B from **step 5**. Let the sample enter the bed completely, then add 300 μL assay buffer and discard the flow-through (*see* **Note 12**). Place the column in a new 15 mL tube. Add 600 μL assay buffer and collect the eluate in ~50 μL fractions (one drop at a time) in appropriate tubes, e.g., 1.5 mL microcentrifuge tubes.
7. Verify the presence of labeled protein in elution fractions by determining their fluorescence intensity and their capillary scan signal shape (*see* Subheading 3.2) in the MST instrument. According to the gel filtration principle, larger particles will

elute prior to smaller particles (*see* **Note 13**). At 20% LED power, 10 nM labeled protein should yield fluorescence intensities of approximately 100–200 counts (*see* **Note 14** and Subheading 3.2).

8. Pool the fractions that contain labeled protein and shield them from light.
9. Determine the protein and dye concentrations and derive the labeling efficiency by measuring the absorbance at 280 (A_{280}) and 650 nm (A_{650}) in a suitable spectrophotometer, e.g., using a NanoDrop instrument (Thermo Scientific) and applying the Lambert-Beer law (*see* **Note 15**).
10. Aliquot the labeled protein as 10 μL aliquots (e.g., into 200 μL PCR tubes), flash-freeze in liquid nitrogen, and store for several weeks to months at −80 °C (*see* **Notes 5** and **16**).

3.1.2 DNA Labeling

1. Design a DNA polynucleotide sequence according to the requirements of the experiment. In this example, a polynucleotide was obtained from a commercial supplier.
2. Design a second complementary polynucleotide sequence, with the addition of a 5' Cy5-label (*see* **Note 17**).
3. In the following steps it is imperative that the samples be shielded from light (kept in the dark) as much as possible to prevent photo bleaching.
4. Combine the single-stranded DNA sequences by mixing 10 nmol of each strand and increase the volume to a total of 100 μL (*see* **Note 18**).
5. Heat the sample to 95 degrees Celsius and let the DNA strands anneal by slowly returning to room temperature. You now have a 100 μM stock of fluorescent double-strand DNA.
6. Verify the integrity of the DNA by running it on a 1% agarose gel, for very short polynucleotides on a 5% polyacrylamide gel (*see* **Note 19**).

3.2 Optimization of Experimental Conditions

Optimization of experimental conditions is paramount to obtain high-quality data and derive accurate binding parameters, which is in particular due the sensitivity of the MST experiment to protein adsorption to exposed surfaces and protein aggregation. To avoid such experimental artifacts, the correct capillary type has to be chosen, and the buffer composition needs to be optimized to ensure a homogeneous state of the sample, free from aggregation. Here we outline this procedure step-by-step (*see* Fig. 2), but we note that some parameters are interrelated and that addition of ligand may result in the need for further optimization.

1. Set the machine to the desired temperature and wait for temperature equilibration (*see* **Notes 20** and **21**).

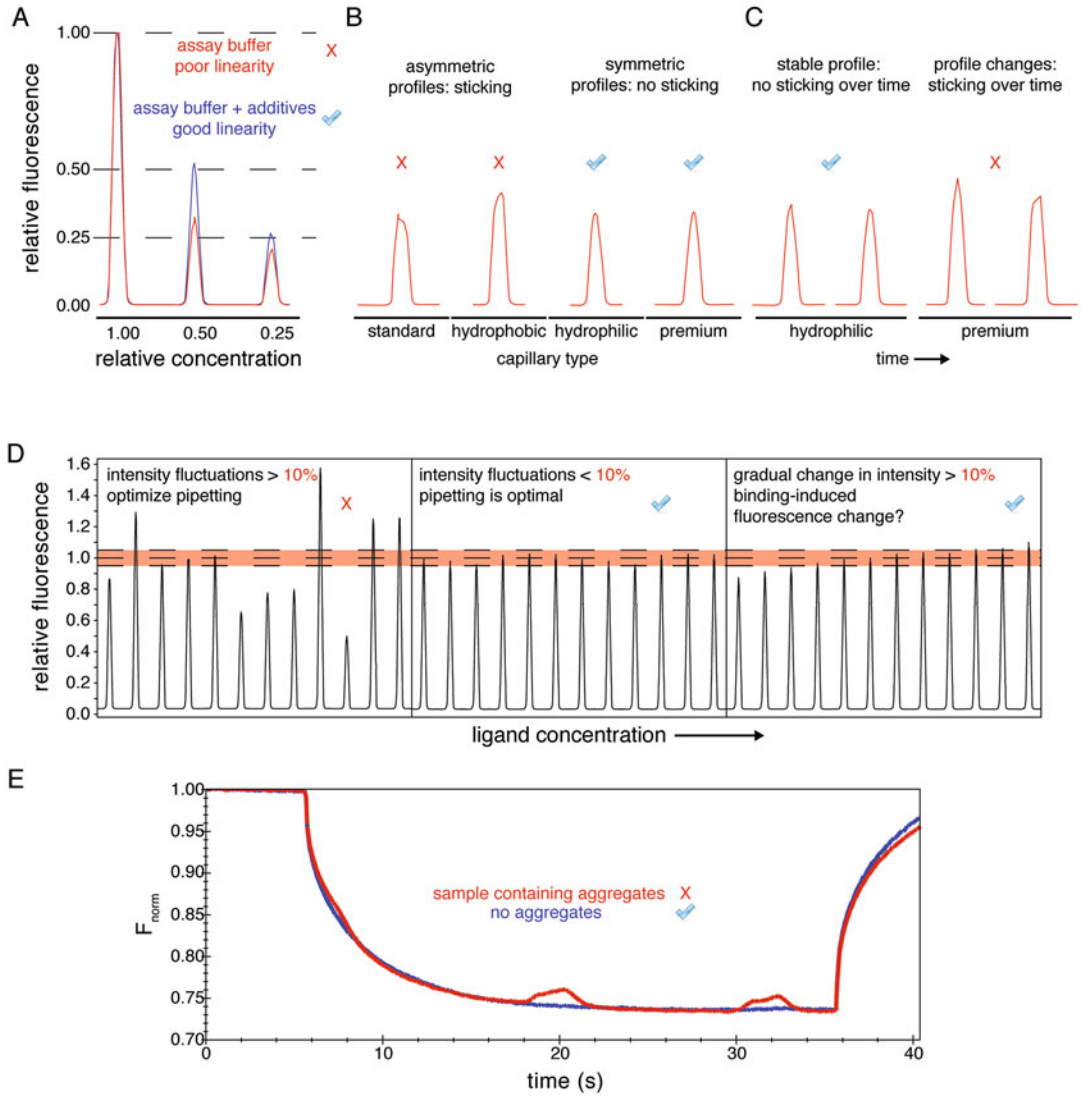

Fig. 2 Optimization of assay conditions (**a**) Capillary scans of a dilution series of the fluorescently labeled molecule. The addition of additives (0.5 mg/mL BSA and 0.05% Tween) prevents sticking to reaction tubes and leads to a consistent dilution series. (**b**) Capillary scans of different types of capillaries loaded with the same labeled molecule. Asymmetric peaks are a sign of adsorption to the capillary wall. (**c**) Time-dependent changes in the capillary scans for the same molecule. While both premium and hydrophilic coatings show no adsorption initially, only hydrophilic capillaries remain free of adsorption. (**d**) Capillary scans of a titration series of the same molecule. Addition of 0.5 mg/mL BSA and 0.05% Tween-20 together with diligent pipetting improves the reproducibility of the fluorescence intensity to within the required limits (compare the left and middle panels). Gradual fluorescence intensity changes are indicative of a binding reaction and can be used for analysis (*see* **Note 36**). (**e**) Aggregates in the sample led to irregularly shaped MST-traces (red), which were prevented by spinning the sample for 20 min at 20,000 × *g* and 4 °C to remove aggregates (*see* **Note 26**) (blue). All data are acquired on NT-467 labeled $APLF^{AD}$ and its interaction with core histone complexes (*see* Subheading 3.6.2)

2. Make a calibration curve of the dye alone at the set temperature. For this purpose prepare 20 μL 200 nM dye solution in assay buffer in a capped, small volume reaction tube to avoid evaporation (e.g., 200 μL PCR tubes) and label this tube 1. Label 8 more PCR tubes 2 through 9. Add 10 μL assay buffer in each tube 2–9. Add 10 μL from tube 1 to 2 and mix by pipetting up and down. Then add with a new pipette tip 10 μL from tube 2 to 3 and mix by pipetting up and down. Continue this series through to tube 9. Fill all samples in standard capillaries (*see* **Note 22**) and perform a capillary scan (button "Start CapScan" in NT Control) at 50% LED power to measure the fluorescence intensity at each concentration. Prepare a calibration curve with fluorescence intensity on the *y*- and dye concentration on the *x*-axis.
3. Determine the optimal concentration of the fluorescently labeled molecule. To this purpose prepare a dilution series using the stock of labeled protein as in **step 2**. Fill the samples in standard capillaries and start the capillary scan with 50% LED power. If the fluorescence is much lower than expected compared to the calibration curve or not linear over the dilution series, the protein likely sticks to the reaction tube or pipette tips (*see* also **step 4**). In that case add of 0.05% Tween-20 or another detergent (*see* Fig. 2a) and repeat the experiment. If the sample behaves well, adjust the concentration to be lower or at most in the order of the expected K_D, while still resulting in a fluorescence signal with high signal-to-noise (*see* **Notes 23** and **24**).
4. Determine the optimal type of capillary coating to ensure a homogenous sample. For this purpose load capillaries of each type (Monolith NT™ Standard, Hydrophobic, Hydrophilic (*see* **Note 4**) and Premium Treated) with working concentration of the labeled biomolecule determined in **step 3** and perform a capillary scan. Inspect the shape of the fluorescence signal, which reflects the distribution of the labeled molecule in a cross-section of the capillary. If a "U"- or "M"-shaped peak is observed instead of a smooth Gaussian-shaped fluorescence peak, the sample adsorbs to the capillary wall (Fig. 2b). Also verify that no sticking occurs over time by running a second capillary scan ~15 min after the first one (*see* Fig. 2c and **Note 25**). For further experiments select capillaries with minimal or no sticking. In case of sticking in all capillary types, proceed to **step 6** and optimize the assay buffer.
5. Use the capillary profiles to also judge the reproducibility of the fluorescence intensity from the four replicates, or from a binding experiment. Random variations larger than 10% can be caused by inaccurate pipetting or sticking to the walls of reaction tubes and pipette tips (Fig. 2d). In that case test whether addition of detergents like Tween-20, passivating agents like

BSA, or higher salt concentrations in the assay buffer improve the results (*see* **Note 26**).

6. Check the thermophoresis signal for sample aggregation. For this purpose start a thermophoresis measurement with the following settings: labeled molecule at working concentration; LED power adjusted to yield at least 200 fluorescence counts; 40% MST power; 30/5 s MST power on/off time. Aggregates, when present, will be transported in and out of the measurement volume, causing sharp increase and decrease in fluorescence over time and a bumpy appearance of the MST curve (Fig. 2e). Make sure to use stocks and buffers that are free from aggregates or particulate matter, and adjust the assay buffer composition to prevent later aggregation (*see* **Note 27**).

3.3 Preparation of Dilution Series

To determine the dissociation constant (K_D) of a molecular interaction, a dilution series of up to 16 titration points is prepared, where the concentration of the fluorescent binding partner is kept constant and the concentration of the unlabeled binding partner is varied (*see* **Notes 28** and **29**).

1. Prepare 200 µL of the fluorescently labeled biomolecule (from Subheading 3.1.1, **step 10**) in the optimized buffer with double the concentration of the final reaction to account for two-fold dilution with titrant (*see* **Note 30**). Here, and in subsequent steps, use small volume reaction tubes to avoid evaporation (e.g., 200 µL PCR tubes).
2. Prepare the titrant stock concentration to be 40-fold the expected K_D (*see* **Note 31**) in assay buffer (labeled tube 1) (*see* **Note 32**) and determine the concentration (*see* **Note 33**).
3. Prepare 15 tubes labeled 2 through 16 with 15 µL of the assay buffer. With a clean tip, transfer 15 µL from tube 1 to tube 2 and mix well by pipetting. Continue this serial dilution until tube 16 (*see* **Note 34**).
4. Transfer 10 µL from tubes 1–16 to new reaction tubes and add 10 µL of your fluorescently labeled sample stock to the tubes (*see* **Note 35**). Mix very well by pipetting up and down. After an adequate incubation time (typically 5 min, *see* **Note 36**), place the capillaries in the tubes to load the samples (*see* **Note 22**).

3.4 MST Measurement

1. Load the capillaries of the previous step in the MST machine (*see* also **Note 21**) and perform a full MST measurement using the LED power setting determined earlier, and two consecutive measurements using 20% and 40% MST power (button "Start CapScan + MST Measurement") (*see* also **Note 25**).
2. Analyze the outcome of the measurement carefully to ensure the data is of sufficient quality. Inspect results of the capillary scan to see if there is ligand-induced sticking; inspect the

reproducibility of the fluorescence intensity to see if the variation is larger than 10% (Fig. 2d, *see* **Note 37**); inspect the MST traces to see if there is ligand-induced aggregation (*see* Fig. 2e). If any of these issues are observed, carefully re-evaluate the previous steps. A new round of assay condition optimization, this time including the ligand, can help to solve these issues. When no issues are encountered, proceed to **step 3**.

3. Analyze the MST-derived binding curve in the MO Affinity Analysis software. If a transition is observed, estimate its amplitude. Estimate the noise from the scatter in the data points at the lowest concentration of ligand where no binding is expected. Minimum amplitude should be 5 units (5‰ normalized fluorescence intensity change) and minimum signal-to-noise should be 3. If either the amplitude or signal-to-noise is too low, increase the MST power to 60–80% (*see* **Notes 38** and **39**).
4. Once the final conditions have been established, perform the serial dilution (Subheadings 3.3, **steps 3** and **4**) in triplicates each with two MST powers of the same dilution series. Next, proceed to data analysis (*see* Subheading 3.5).

3.5 MST Data Analysis

The manufacturer's MO Affinity Analysis software provides multiple options to extract a binding curve from the raw MST traces (*see* **Note 40**). The resulting binding curves can be fit directly in the software for a 1:1 binding model, or the data can be exported to be used in third-party software. Here we describe the default procedure using the instrument software, together with options for custom analysis (*see* **Note 41**).

1. In a new analysis set, click and drag the three replicates in a single experiment for a combined analysis.
2. If binding-induced changes in fluorescence intensity are observed, fit the binding curve using the "Initial Fluorescence" button (*see* also **Note 37**). Otherwise, proceed to **step 3**.
3. Extract replicate-averaged binding curves using the two default settings: (1) "Thermophoresis + T-Jump"; (2) "Thermophoresis," and fit these using the thermodynamic model to extract the K_D (*see* **Note 42**). Compare the extracted values for consistency.
4. Use the "Temperature Jump" method to see if there is a binding-induced change in the fluorophore, which may hold structural information if the location of the fluorophore is known.
5. Export the data for further analysis, error estimation of fit--parameters or fitting to custom-binding models using, e.g., MatLab (scripts available upon requests), Python, or the PALMIST program of Scheuermann et al. [18].

3.6 Description of Examples

3.6.1 Different DNA Compaction Modes of HMfB

HMfB is an archaeal histone protein from *Methanothermus fervidus* with a sequence-dependent ability to either bend or wrap DNA [19, 20]. Here, we analyzed the HMfB-DNA interaction using two DNA sequences (78 bp), either with a specific HMfB-binding site ("specific sequence") or without ("aspecific sequence"). Premium capillaries were used as reduced affinity was observed for the regular and hydrophobic capillaries, likely due to the protein sticking to the capillaries. The F_{norm} values derived from the MST traces were normalized to obtain ΔF_{norm} values to facilitate comparison (Fig. 3a, b). Note that a custom dilution series was made to better sample the transitions regions.

For the aspecific sequence a single binding transition is observed that can be fit yielding a K_{D} of 1 ± 0.2 μM (Fig. 3b). For the specific DNA sequence two transitions are observed. The ΔF_{norm} decreases at low protein concentrations, indicating that the bound DNA is more mobile than free DNA. At higher protein concentrations however, the ΔF_{norm} increases indicating a less mobile, and possibly larger protein-DNA complex. This second binding mode occurs at concentrations identical to those found for aspecific DNA, indicating that this is an aspecific DNA-binding mode. Together, this suggests that at high protein concentrations, HMfB forms the same structure independent of DNA sequence, while at low protein concentrations it forms a more compact structure at specific sequences. This hypothesis is supported by data from complementary techniques (such as TPM described in Chapter 14), and summarized in Fig. 3c.

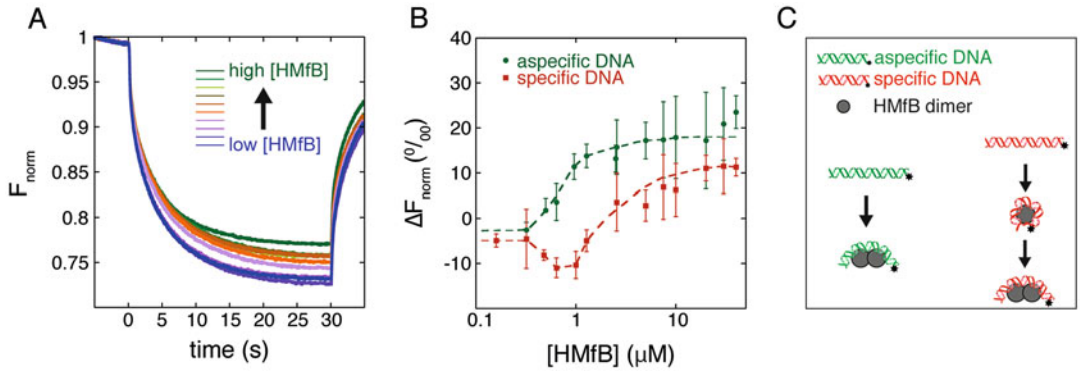

Fig. 3 MST analysis of HMfB interaction with two DNA substrates (**a**) MST-thermophoresis curves for a range of HMfB concentrations. Data acquired at 22 °C, 40 nM of Cy5-labeled DNA in 50 mM Tris–HCl pH 8.0, 75 mM KCl, premium capillaries, 20% laser power, 40% MST power. (**b**) Change in normalized fluorescence (ΔF_{norm}) for HMfB binding to a specific (red) or aspecific DNA sequence. Error bars indicate the standard deviation in a triplicate of experiments. (**c**) Model depicting the possible conformations of the HMfB-DNA complex. Without a specific binding site in the DNA substrate, HMfB binds as a multimer, forming a large structure. If a preferred DNA sequence is present, HMfB forms first a compact nucleosome-like structure. At higher HMfB concentrations similar structures as seen for the aspecific DNA sequence can be formed

3.6.2 Histone Binding by Histone Chaperone APLF

Histone chaperones are involved in the assembly and disassembly of the nucleosome for DNA replication, transcription, and repair [21]. Aprataxin and Polynucleotide kinase Like Factor (APLF) is a DNA repair protein with histone chaperone function [22]. Here, we studied the interaction of the APLF acidic domain ($APLF^{AD}$) with histone complexes using MST. $APLF^{AD}$ was labeled with the manufacturer's red dye NT-647 according to Subheading 3.1.1. Given the low labeling efficiency (~15%) and the expected high affinity, 25 nM of $APLF^{AD}$ was used with 100% LED power to arrive at an optimal fluorescence intensity of 400 counts. The assay buffer was supplemented with both 0.5 mg/mL BSA and 0.05% Tween-20 and experiments were conducted in hydrophilic-treated capillaries to prevent sticking to the reaction tubes and the capillaries (*see* Fig. 2).

The MST data show that $APLF^{AD}$ binds with high and comparable affinity to both H2A-H2B and $(H3\text{-}H4)_2$, suggesting that APLF is a generic histone chaperone (Fig. 4). Interestingly, the binding curves show in both cases two transitions, suggesting two separate binding events (*see* **Note 43**), one with affinity in the higher nanomolar range and one in the micromolar range. The data were fitted to a sequential binding site model using an in-house written MatLab script. Errors in the best-fit parameters represent the 95% confidence interval based on statistical F-tests [18]. The additional binding mode of histones to $APLF^{AD}$ may be relevant in its chaperoning mechanism, promoting the retention of multiple copies of histone complexes.

3.6.3 Binding of a Nucleosome-Mimicking Peptide to a Reader Protein

Posttranslational histone modifications are key regulators of chromatin function, mostly through their specific interaction with so-called reader proteins. We recently found that the recognition of trimethylated lysine 36 on H3 (H3K36me3) by the PSIP1-PWWP domain is driven by the nucleosomal context of this modification [23]. PSIP1-PWWP binds with very low affinity (K_D 17 mM) to a H3K36me3 peptide, but with 10,000-fold enhanced affinity to modified nucleosomes [23]. To address the importance of electrostatics, we here investigate by MST the binding of PSIP1-PWWP to a $H3K_C36me3$ peptide modified with a stretch of glutamate residues ($H3K_C36me3\text{-}E_7$) to mimic nucleosomal DNA. NanoTemper dye NT-647 was coupled to a cysteine mutant of PSIP1-PWWP (N86C). Premium capillaries and 0.05% Tween-20 were used to avoid fluorescence loss due to sticking.

The capillary scan of the titration series showed a ligand-dependent decrease in initial fluorescence, only for the trimethylated version of the peptide and not for an unmodified peptide (Fig. 5a). Additionally, a denaturing test (*see* **Note 37**) showed full fluorescence recovery, proving that the changes are binding

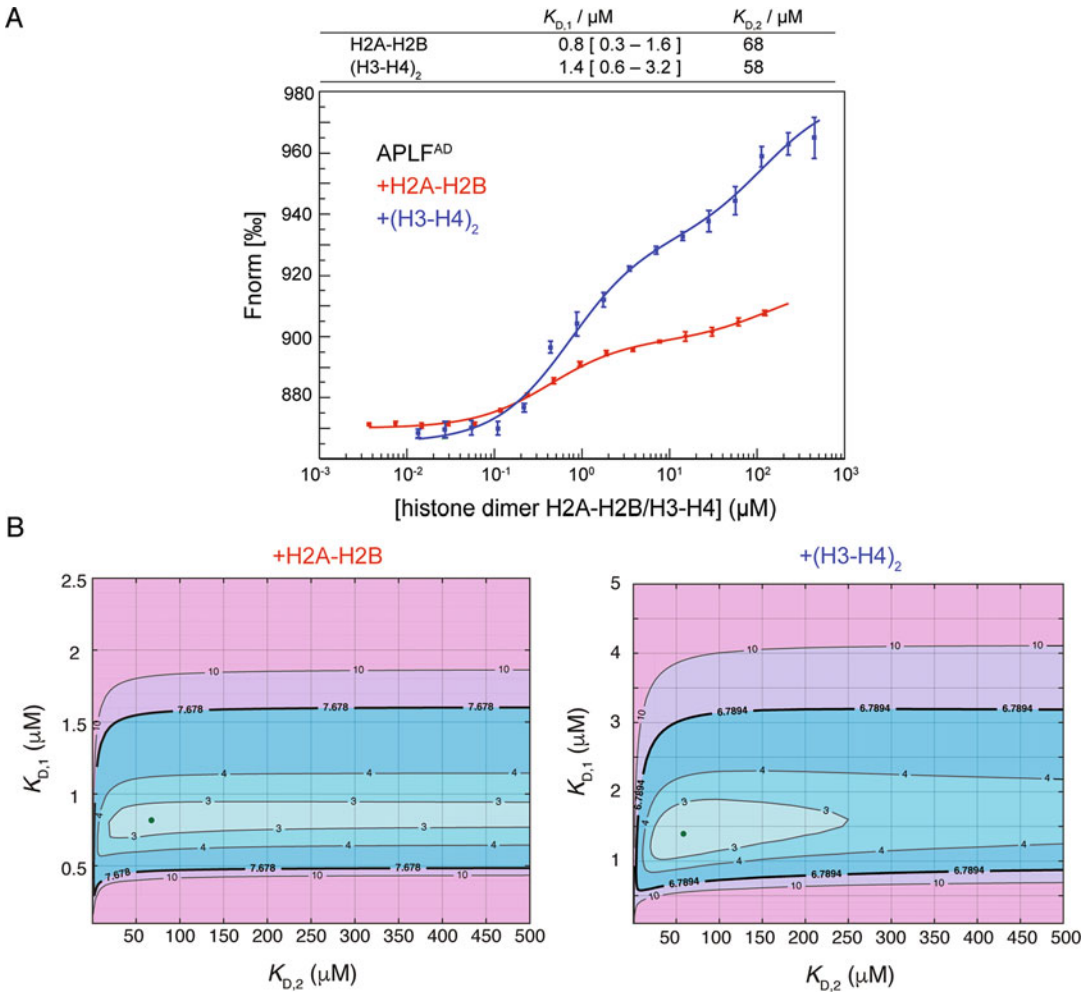

Fig. 4 APLF^{AD} binds with similar affinities to H2A-H2B and (H3-H4)$_2$. (**a**) MST-binding curves of H2A-H2B (red) or (H3-H4)$_2$ (blue) with fluorescently labeled APLF^{AD} (25 nM) in assay buffer (25 mM NaPi, pH 7.0, 300 mM NaCl, supplemented with 0.5 mg/mL BSA and 0.05% Tween-20), recorded at 25 °C, 20% MST, and 100% LED power with 30/5 s laser-on/off time. The binding curve represents the average from three measurements with standard deviation. Best-fit values for the corresponding affinities and 95% confidence limits are listed in the table. (**b**) Plots showing the reduced χ^2-surface that expresses the quality of fit in contour-mode as a function of the high-affinity ($K_{D,1}$) and the low-affinity ($K_{D,2}$) dissociation constants for H2A-H2B (left) and (H3-H4)$_2$ (right) binding to APLF^{AD}. The best-fit values are indicated by a green dot. The 95% confidence critical value for the reduced χ^2 is indicated with a thick black line. Figure reproduced from ref. 30 with permission from the authors

induced. Fits of the initial fluorescence, T-jump, and thermophoresis + T-jump all give comparable and consistent K_D values of ~1.6 mM (Fig. 5b, c, d). The tenfold increase in binding affinity compared to the native H3K36me3 peptide underscores the importance of the nucleosomal context, in which both electrostatic and geometric factors are critical.

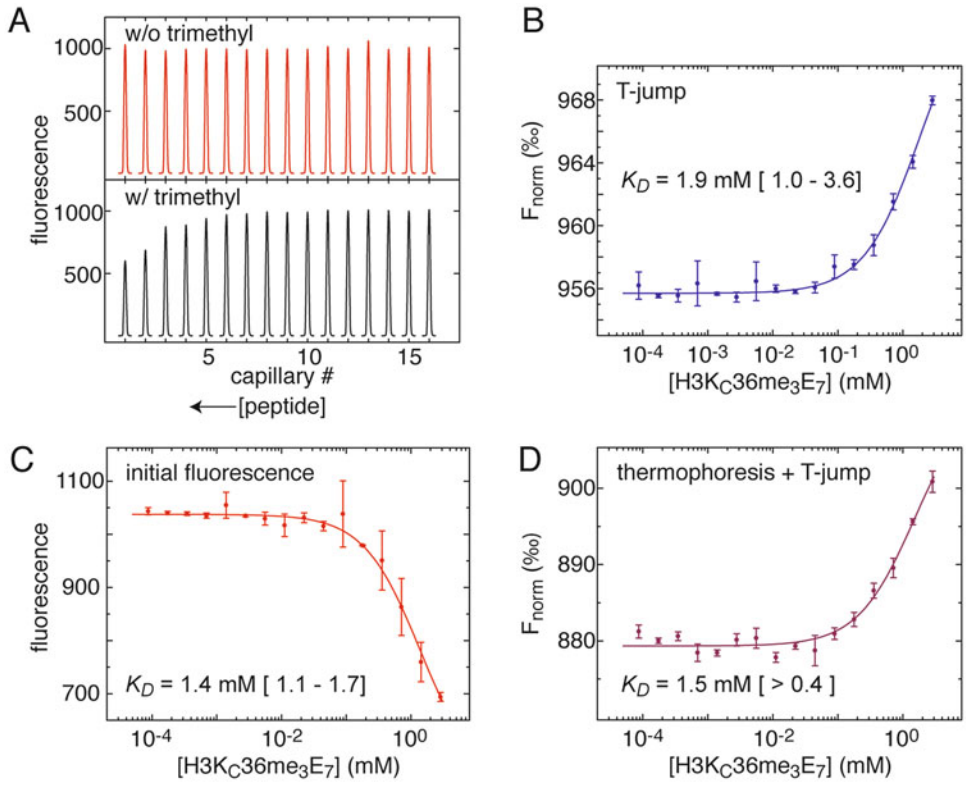

Fig. 5 MST of nucleosome-mimicking H3K$_C$36me3-peptides binding to the PSIP1-PWWP domain. (**a**) Capillary scans for H3K$_C$36-E$_7$ peptides (SAPATGGVCKEEEEEEE) with (red) and without (black) cysteine-based trimethyl lysine analogue [31]. (**b**, **c**, **d**) Analysis of the MST measurements was done by fitting the data for T-jump (**b**), initial fluorescence (**c**) and Thermophoresis + T-jump (**d**). Best-fit values for the K_D and 95% confidence limits are indicated in the plots. Data recorded on 0.35 μM NT-467 labeled N86C PWWP domain titrated with peptide in 10 mM Tris pH 7.5, 100 mM KCl, supplemented with 0.05% Tween-20, 25 °C, 20%/20% LED/MST power, with 30/5 s laser-on/off time

3.6.4 Analysis of a Nucleosome-Peptide Interaction

The latency-associated nuclear antigen (LANA) of Kaposi's sarcoma-associated herpes virus (KHSV) binds to nucleosomes to ensure the persistence of the KHSV cosmid in both daughter cells during host cell division [24]. A short peptide sequence from LANA binds strongly and specifically to the acidic patch on the H2A-H2B surface of the nucleosome [25]. Here, we analyzed the binding of a peptide containing the residues 2–22 of LANA (2.1 kDa) to nucleosomes (210 kDa), which were labeled using Nano Temper's NT467-Red-NHS dye after reconstitution [26]. Labeling efficiency was on the order of 10%, sufficient to yield 600 fluorescence counts with a 135 nM solution and 100% LED power. Labeling and purification did not interfere with nucleosome integrity as shown by native PAGE analysis (data not shown). Optimization of the conditions led to the choice of 0.1 mg/mL BSA as additive—0.01% Triton X-100 or 0.01%

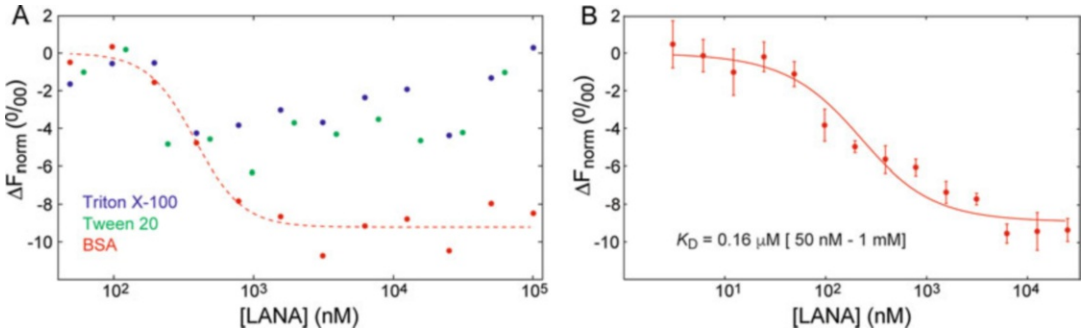

Fig. 6 MST of mononucleosomes binding to LANA. (**a**) Buffer optimization: comparison of the binding curves of 200 nM NT-467 labeled nucleosomes titrated with LANA in 10 mM Tris pH 7.5, 100 mM KCl, supplemented with either BSA, Tween-20 or Triton X-100. A fit to the BSA curve is shown to guide the eye. (**b**) MST-binding curve (average of three independent measurements, with standard deviations) of 135 nM of NT-467 labeled mononucleosomes titrated with LANA. Measurements were performed at 22 °C, 50% MST and 100% LED power with 30/5 s laser-on/off time. Best-fit values and 95% confidence intervals are shown in the figure

Tween 20 resulted in comparatively weaker thermophoretic changes upon LANA binding (Fig. 6a). Hydrophobic capillaries were selected to prevent binding-induced sticking.

The MST-binding curves show a clear transition that was fitted using an in-house written MatLab script to a single binding event with K_D of 0.16 μM, which agrees well with the previously published value of 0.24 μM under slightly different conditions [27] (Fig. 6b). These data demonstrate the possibility of reliably determining binding parameters of small molecule effectors to fluorescently labeled nucleosomes. While the thermophoretic changes may be larger using the reverse labeling setup, the current strategy allows screening of several effectors with minimum nucleosome consumption.

4 Notes

1. One is by no means restricted to use the manufacturer's fluorescent labeling kit. There are many commercially available fluorescent compounds that can be coupled to free amino or thiol groups. Make sure to use compounds compatible with the excitation and detection wavelengths of your instrument.
2. Assay buffer refers to the buffer of choice in which the interaction is investigated. The protein should be stable and well behaved in this buffer. Typical buffer conditions are 50 mM Tris–HCl pH 7.4, 150 mM NaCl, 10 mM $MgCl_2$, 0.05% Tween-20.
3. We limit the description of the method to the Monolith NT.115 instrument from NanoTemper Technologies

(Munich, Germany). Instruments with either a higher fluorescence sensitivity, a setup to excite and detect intrinsic tryptophan fluorescence, or a high-throughput automated screening setup are also available.

4. Hydrophilic-treated capillaries were used in this study, but these are no longer available. Premium capillaries are advised as replacement.
5. Higher stock concentrations are useful to have optimum flexibility to adjust exact assay buffer composition during optimization of the experimental conditions (*see* Subheading 3.2) or in follow-up experiments.
6. In case no binding is detected with one binding partner fluorescently labeled, it is useful to try and test labeling the other binding partner.
7. Buffer exchange to labeling buffer (**steps 2** and **3**) can be skipped if the protein sample is purified directly into a suitable buffer (good buffers are HEPES, PBS, Na-Ac) with $6.5 < \text{pH} < 8.5$. Buffers should not contain reducing agents dithiothreitol (DTT) and β-mercaptoethanol (BME), since these substances significantly reduce labeling efficiency. Tris (2-carboxyethyl)phosphine (TCEP) can be used as a reducing agent if required. Additionally, the buffer for NHS-labeling must be free of primary amines, e.g., ammonium ions, Tris, glycine, ethanolamine, glutathione or imidazole. Buffers with protein impurities or protein carriers like bovine serum albumin (BSA) should not be used. If a labeling buffer is used other than the one supplied, dye concentrations required for optimum labeling efficiency may need to be re-established.
8. The dye can be used for a few hours after resuspending it according to the manufacturer's manual. For longer storage of stock solutions, dye may be frozen and aliquoted in DMSO under anhydrous conditions to prevent hydrolysis.
9. For some samples labeling efficiency may be increased by using a higher fold excess of dye.
10. The reaction can be incubated in a drawer or cupboard, or wrapped in aluminum foil.
11. For optimal MST results, unreacted dye needs to be removed.
12. When using 200 μL labeling reaction, the volume must be adjusted to 500 μL after the sample has entered the bed by adding 300 μL assay buffer. If a scale up or scale down of the reaction is necessary, make sure the total volume loaded on the column is of 500 μL. Ensure the whole labeling mix has entered the column bed before completing to 500 μL
13. Use the early fractions that contain higher amounts of labeled protein. Depending on the assay buffer composition, later

fractions might contain free dye. It can also be helpful to look at the thermophoresis signal and check for "bumps," which are indicative of aggregates in the sample (*see* Fig. 2d).

14. If required, after fluorescent labeling, the protein can be concentrated using a device like an Amicon® Ultra Centrifugal Filter (Millipore).
15. The molar absorbance of the dye at 650 nm is 250,000 M^{-1} cm^{-1}. Protein absorption at 280 nm has to be adjusted according to $A_{protein} = A_{280}–0.028 \cdot A_{650}$ due to absorption of the dye. Typically, the labeling ratio is between 0.5 and 1.1 (according to the manufacturer).
16. If the stored protein is to be used for a new interaction study, repetition of previous experiments can be conducted to assess the stability and quality of the sample.
17. It is possible to generate much larger labeled DNA sequences for MST using Polymerase Chain Reaction (PCR), by following the protocol described in Chapters 12 and 14 using fluorescently labeled DNA sequences as primers.
18. You can make the DNA stock at any concentration. Making a higher concentration stock allows you to reduce the effects of incidental photo bleaching.
19. If in your control step you do not observe a single band for your double-stranded DNA, you should redo the annealing of the two strands while reducing the rate at which the two DNA strands anneal.
20. The experimental temperature in the MST instrument can be set between 22 and 45 °C or left unspecified for room temperature. The temperature is best set to a defined value and reported, together with the used MST power.
21. After opening of the instrument's front door for sample insertion, close the door and wait until the set temperature is reached as shown on the instrument's display.
22. Both tube and capillary can be tilted to ease filling. To have air on both sides, the capillary may be inverted for 1 or 2 s after loading.
23. Typically, 5–100 nM of the fluorescently labeled molecule is sufficient to obtain optimal fluorescence, with intensity above 400 and below 1500, with a minimum of 200. The LED power can be varied between 15% and 95% to achieve this. For very high-affinity interactions, use the lowest possible concentration in which you get 200 fluorescence counts with 95% LED power.
24. If the concentration of labeled molecule is on the order of the K_D, the dilution series (Subheading 3.3) is better prepared

linearly to optimally sample the binding curve, in which case the data is best plot using a linear *x*-axis resulting in a hyperbole-binding curve.

25. Capillary scans of each new titration should be performed at the start of the experiment to assess the quality of the samples and again at the end of the experiment to check for changes in the fluorescence peak shape and intensity that can occur over time.
26. Additives should be used at the lowest functional concentration possible, as they may affect the binding.
27. Aggregates can be removed by centrifuging sample stocks (20 min, 20,000 × *g*, 4 °C) and filter buffers through 0.22–0.45 μm filters. Detergents such as Tween 20 or Triton X-100 (0.01–0.1%) or changes in assay buffer conditions (different ionic strength, pH) can also help to prevent aggregation or binding-induced aggregation.
28. A control experiment can be conducted with an unrelated nonbinding molecule or a binding-deficient mutant of the binding partner.
29. Do not use less than 10 titration points per experiment.
30. Using a two-fold serial dilution, which is easily performed with minimum source of error, optimally spaced data points along the sigmoidal-binding curve are obtained (*see* also **Note 24**).
31. The "Concentration Finder" tool within the NT Control software can be used to simulate binding curves and determine the required titrant concentration ranges. In case the dissociation constant is unknown, a 3–5 fold dilution series starting from a high (~100 μM) concentration will allow monitoring of binding events within a ligand concentration range of nM to μM. If a binding transition is observed, the titrant stock concentration and dilution series can be adjusted accordingly.
32. If the sample buffer is different from the assay buffer, adjust the composition of the buffers in order to obtain same composition (e.g., DMSO, glycerol, salt, detergent, BSA etc.) by adding the components in the stock preparations to the final concentration needed.
33. As in any quantitative essay it is essential to accurately determine protein concentration, work with calibrated pipettes, and perform precise and reproducible protein dilution.
34. Change the pipet tip after each transfer or, alternatively, pre-wet the tip properly. For some pipettes it may be necessary to reset the pipetting volume after placing a new pipet tip.

35. After having obtained practical experience and confidence with the pipetting procedure, the pipetting volumes can be reduced to half to save material.
36. The incubation time is necessary to establish equilibrium which is determined by the binding kinetics of complex formation and dissociation. In sporadic cases with very high affinity and very low dissociation rates, equilibration may take hours to days [18]. Equilibration can be verified by repeating a titration series after different incubation times, e.g., 1, 5, and 10 min.
37. A systematic ligand-dependent increase or decrease in fluorescence intensity may be caused by binding if the fluorophore is close to the binding site. To determine if this is the case, spin down the reaction tubes for 10 min at 15,000 × *g*, remove 10 μL of supernatant, and add this to 10 μL of denaturing buffer (4% SDS, 40 mM DTT), then heat for 5 min at 95 °C, load the samples into capillaries and perform a capillary scan. If the fluorescence intensity is now constant within 10%, the effect was binding-induced. If the effect remains, the sample may be lost due to aggregation and a new round of optimization has to be started.
38. Reduce the laser-on time at high MST powers to 15 s to reduce effects from sample-heating.
39. Compare refs. 18, 28, 29 for MST curves with a range of signal-to-noise ratios.
40. Sign and amplitude of the thermophoresis effect are typically not analyzed since they depend in a complex manner on the changes in conformation, size, and charge.
41. The use of custom software permits more realistic determination of errors in fit-parameters and flexibility in choosing binding models.
42. Avoid the use of the Hill equation, since the reported EC50 values are protein concentration dependent and the fitted cooperativity coefficient may be larger than the number of binding sites.
43. In case multiple binding transitions are observed in an MST titration, it can be useful to confirm the result by using complementary techniques.

Acknowledgments

We thank the NanoTemper team for their support and advice. We thank prof. Dr. G.A. van der Marel and N. Meeuwenoord (Leiden University) for support in peptide synthesis and purification. This work was supported by the Netherlands Organisation for Scientific

Research (NWO) (VIDI 864.08.001, VICI 016.160.613 to RTD and VIDI 723.013.010 to HvI) and NanonextNL of the Government of the Netherland and 130 partners.

References

1. Ludwig C (1856) Diffusion zwischen ungleich erwärmten Orten gleich zusammengesetzter Lösungen. Sitzungsber Akad Wiss Wien Math-Naturwiss 20:539
2. Wienken CJ, Baaske P, Rothbauer U et al (2010) Protein-binding assays in biological liquids using microscale thermophoresis. Nat Commun 1:100. https://doi.org/10.1038/ncomms1093
3. Duhr S, Braun D (2006) Why molecules move along a temperature gradient. Proc Natl Acad Sci U S A 103:19678–19682. https://doi.org/10.1073/pnas.0603873103
4. Seidel SAI, Dijkman PM, Lea WA et al (2013) Microscale thermophoresis quantifies biomolecular interactions under previously challenging conditions. Methods 59:301–315. https://doi.org/10.1016/j.ymeth.2012.12.005
5. Jerabek-Willemsen M, André T, Wanner R et al (2014) MicroScale Thermophoresis: interaction analysis and beyond. J Mol Struct 1077:101–113. https://doi.org/10.1016/j.molstruc.2014.03.009
6. Schubert T, Pusch MC, Diermeier S et al (2012) Df31 protein and snoRNAs maintain accessible higher-order structures of chromatin. Mol Cell 48:434–444. https://doi.org/10.1016/j.molcel.2012.08.021
7. Zillner K, Filarsky M, Rachow K et al (2013) Large-scale organization of ribosomal DNA chromatin is regulated by Tip5. Nucleic Acids Res 41:5251–5262. https://doi.org/10.1093/nar/gkt218
8. Su X-C, Wang Y, Yagi H et al (2014) Bound or free: interaction of the C-terminal domain of Escherichia coli single-stranded DNA-binding protein (SSB) with the tetrameric core of SSB. Biochemistry 53:1925–1934. https://doi.org/10.1021/bi5001867
9. Silva APG, Ryan DP, Galanty Y et al (2016) The N-terminal region of Chromodomain helicase DNA-binding protein 4 (CHD4) is essential for activity and contains a high mobility group (HMG) box-like-domain that can bind poly(ADP-ribose). J Biol Chem 291:924–938. https://doi.org/10.1074/jbc.M115.683227
10. Yamagata K, Kobayashi A (2017) The cysteine-rich domain of TET2 binds preferentially to mono- and dimethylated histone H3K36. J Biochem 161:327–330. https://doi.org/10.1093/jb/mvx004
11. Zillner K, Jerabek-Willemsen M, Duhr S et al (2012) Microscale thermophoresis as a sensitive method to quantify protein: nucleic acid interactions in solution. Methods Mol Biol 815:241–252. https://doi.org/10.1007/978-1-61779-424-7_18
12. Zhang W, Duhr S, Baaske P, Laue E (2014) Microscale thermophoresis for the assessment of nuclear protein-binding affinities. Methods Mol Biol 1094:269–276. https://doi.org/10.1007/978-1-62703-706-8_21
13. Flores JK, Kariawasam R, Gimenez AX et al (2015) Biophysical characterisation and quantification of nucleic acid-protein interactions: EMSA, MST and SPR. Curr Protein Pept Sci 16:727–734
14. Schubert T, Längst G (2015) Studying epigenetic interactions using MicroScale Thermophoresis (MST). AIMS Biophysics 2 (3):370–380
15. Willhoft O, McCormack EA, Aramayo RJ et al (2017) Crosstalk within a functional INO80 complex dimer regulates nucleosome sliding. elife 6:e25782. https://doi.org/10.7554/eLife.25782
16. Schrader A, Gross T, Thalhammer V, Längst G (2015) Characterization of Dnmt1 binding and DNA methylation on nucleosomes and Nucleosomal arrays. PLoS One 10:e0140076. https://doi.org/10.1371/journal.pone.0140076
17. Zocco M, Marasovic M, Pisacane P et al (2016) The Chp1 chromodomain binds the H3K9me tail and the nucleosome core to assemble heterochromatin. Cell Discovery 2:16004. https://doi.org/10.1038/celldisc.2016.4
18. Scheuermann TH, Padrick SB, Gardner KH, Brautigam CA (2016) On the acquisition and analysis of microscale thermophoresis data. Anal Biochem 496:79–93. https://doi.org/10.1016/j.ab.2015.12.013
19. Bailey KA, Marc F, Sandman K, Reeve JN (2002) Both DNA and histone fold sequences contribute to archaeal nucleosome stability. J Biol Chem 277:9293–9301. https://doi.org/10.1074/jbc.M110029200

20. Henneman B, Dame RT (2015) Archaeal histones: dynamic and versatile genome architects. AIMS Microbiol 1:72–81
21. Hammond CM, Strømme CB, Huang H, et al (2017) Histone chaperone networks shaping chromatin function. Nat Publ Group 1–19. doi: https://doi.org/10.1038/nrm.2016.159
22. Mehrotra PV, Ahel D, Ryan DP et al (2011) DNA repair factor APLF is a histone chaperone. Mol Cell 41:46–55. https://doi.org/10.1016/j.molcel.2010.12.008
23. van Nuland R, van Schaik FM, Simonis M et al (2013) Nucleosomal DNA binding drives the recognition of H3K36-methylated nucleosomes by the PSIP1-PWWP domain. Epigenetics Chromatin 6:12. https://doi.org/10.1186/1756-8935-6-12
24. Ballestas ME, Chatis PA, Kaye KM (1999) Efficient persistence of extrachromosomal KSHV DNA mediated by latency-associated nuclear antigen. Science 284:641–644
25. Barbera AJ, Chodaparambil JV, Kelley-Clarke B et al (2006) The nucleosomal surface as a docking station for Kaposi's sarcoma herpesvirus LANA. Science 311:856–861. https://doi.org/10.1126/science.1120541
26. Dyer PN, Edayathumangalam RS, White CL et al (2004) Reconstitution of nucleosome core particles from recombinant histones and DNA. Meth Enzymol 375:23–44
27. Beauchemin C, Moerke NJ, Faloon P, Kaye KM (2014) Assay development and high-throughput screening for inhibitors of Kaposi's sarcoma-associated Herpesvirus N-terminal latency-associated nuclear antigen binding to nucleosomes. J Biomol Screen 19:947–958. https://doi.org/10.1177/1087057114520973
28. Allam R, Scherbaum CR, Darisipudi MN et al (2012) Histones from dying renal cells aggravate kidney injury via TLR2 and TLR4. J Am Soc Nephrol 23:1375–1388. https://doi.org/10.1681/ASN.2011111077
29. van der Berg JP, Madoori PK, Komarudin AG et al (2015) Binding of the Lactococcal drug dependent transcriptional regulator LmrR to its ligands and responsive promoter regions. PLoS One 10:e0135467. https://doi.org/10.1371/journal.pone.0135467
30. Corbeski I, Dolinar K, Wienk H, et al (2018) DNA repair factor APLF acts as a H2A-H2B histone chaperone through binding its DNA interaction surface. Nucleic Acid Res. https://doi:10.1093/nar/gky507
31. Simon MD, Chu F, Racki LR et al (2007) The site-specific installation of methyl-lysine analogs into recombinant histones. Cell 128:1003–1012. https://doi.org/10.1016/j.cell.2006.12.041